

CRYSTAL STRUCTURE OF A MONOCLINIC PYRRHOTITE (Fe_7S_8)

MASAYASU TOKONAMI,¹ KATSUHISA NISHIGUCHI² AND NOBUO MORIMOTO,³ *Institute of Scientific and Industrial Research, Osaka University, Suita, Osaka 565, Japan.*

ABSTRACT

The crystal structure of the monoclinic $4C$ -type pyrrhotite (Fe_7S_8) has been refined using the three-dimensional intensity data collected with Zr filtered MoK_α radiation from an untwinned crystal from Kisbanya, Rumania. This crystal has the cell dimensions of $a = 11.902 \pm 0.008$, $b = 6.859 \pm 0.005$, $c = 22.787 \pm 0.010$ Å, and $\beta = 90^\circ 26' \pm 3'$. It was refined in space group $F2/d$ and the final weighted R factor is 0.045 for 487 crystallographically independent reflections.

The structure obtained confirms the ordered arrangement of vacant positions for iron atoms proposed by Bertaut (1953), and gives shifts of iron and sulfur atoms from the atomic positions in the ideal NiAs -type structure. All iron atoms lie between six sulfur atoms with octahedral arrangements and also between a few iron atoms which must be considered to be the nearest neighbors because of short Fe—Fe distances. The mean Fe—S bond lengths in the four FeS_6 octahedra are 2.446, 2.456, 2.449, and 2.444 Å, and the Fe—Fe distances are 2.868, 2.911, and 2.956 Å along the c axis. In the iron layer normal to the c axis, one of the Fe—Fe distance is 2.944 Å, though the others are more than 3.1 Å. The group of seven iron atoms along the c axis can be considered as a collective unit in the $4C$ -type pyrrhotite as the triangular group in the troilite structure. Each iron group is connected with two others through the short Fe—Fe bonds in the basal iron layers.

The atomic arrangements around the vacant positions for iron atoms show slight contraction of the vacant space in comparison with the space around iron atoms.

INTRODUCTION

Pyrrhotite (Fe_{1-x}S) has been extensively studied, because of the importance and complexity of its phase relations, structures, and magnetic properties. A detailed review on the studies of the properties and structures of pyrrhotite has been given by Ward (1970). Five different types of pyrrhotite have been confirmed to be stable at room temperature by studying single crystals of natural pyrrhotite (Morimoto, Nakazawa, Nishiguchi, and Tokonami, 1970; Morimoto, Naka-

¹ Present address: Fachbereich Geowissenschaften; Mineralogie, Kristallographie, Petrologie, Philipps-Universität, 355 Marburg/Lahn, Deutschhausstr. 10, Germany.

² Present address: Industrial Research Institute of Chiba Prefecture, Chiba 280, Japan.

³ To whom all the correspondence should be addressed.

zawa, Tokonami, and Nishiguchi, 1971). The five types are superstructures of the NiAs-type structure, with cell dimensions A , about 3.45 Å; C about 5.8 Å; and have essentially stoichiometric compositions, $Fe_{n-1}S_n$ ($n \geq 8$), with the structures of $(n/2)C$ type for n even and of nC type for n odd (Morimoto, Nakazawa, Nishiguchi, and Tokonami, 1970). Three new types of pyrrhotite stable at high temperatures were also described by Nakazawa and Morimoto (1971).

Monoclinic pyrrhotite of the $4C$ -type superstructure occurs in nature at and near the composition Fe_7S_8 , with $a = 2\sqrt{3}A$, $b = 2A$, and $c = 4C$, and $\beta = 90.4^\circ$. On the basis of geometry of the diffraction patterns of twinned crystals of this pyrrhotite, Bertaut (1953) proposed that the superstructure contained ordered vacancies in alternate iron layers normal to the c axis. The space group and cell dimensions determined by him, were recently confirmed by Corlett (1968) and Wuensch (Ward, 1970) using untwinned crystals. However, there was no report on the crystal structure of the monoclinic $4C$ -type pyrrhotite based on the comparison of the observed and calculated structure factors, though the structure of troilite (FeS) was determined by Bertaut (1956) and refined by Evans (1970) and that of the hexagonal $3C$ -type was determined by Fleet (1971).

The present investigation has been initiated to describe the crystal structure of the monoclinic $4C$ -type pyrrhotite using the three-dimensional counter-measured intensities and to elucidate the arrangement of vacant positions for iron atoms and the effects of the vacancies on the shifts of iron and sulfur atoms from the ideal NiAs structure. The characteristics of complex magnetic and electric properties of the pyrrhotite can be explained based only on the precise crystal structure.

EXPERIMENTAL

Many crystals of monoclinic pyrrhotite from various localities were examined by the X-ray single crystal method to find single crystals for structure determination. The crystals examined were in twin relations by 60° or 120° rotation about the pseudo-hexagonal c^* axis. Crystals from Kisbanya, Rumania were also examined, which had been described by Corlett (1968) and given to us by her. Though the crystals also showed the twin relations, a small platy fragment with $0.03 \times 0.03 \times 0.01$ mm was found to be untwinned, and used for intensity collection throughout in this study. All attempts to obtain larger single crystals than this specimen were not successful.

If we assume symmetry centers in the structure of the pyrrhotite, the possible space group is $C2/c$, which was conveniently expressed as $F2/d$ by Bertaut (1953) to keep an approximate orthogonal relation between the axes. This centrosymmetric space group was adopted during the structure determination and successful refinement of the structure confirmed this choice. The cell dimensions were determined from the goniometry of the reciprocal lattice points 12.4.0, 6.6.0, and 0.0.32 using the Rigaku four-circle automatic diffractometer with $Mo-K\alpha_1$ radiation ($\lambda = 0.70929$

Å). Based on space group $F2/d$, they are $a = 11.902 \pm 0.008$, $b = 6.859 \pm 0.005$, $c = 22.787 \pm 0.010$ Å, and $\beta = 90^\circ 26' \pm 3'$ in good agreement with the values obtained previously (Corlett, 1968; Wuensch, 1969). The estimated standard deviations of the cell dimensions were obtained by the relative errors derived from the equation, $2d \sin \theta = n\lambda$, considering possible errors in reading of angles. The calculated density of this specimen is $4.62 \text{ g}\cdot\text{cm}^{-3}$ for eight Fe_7S_8 units in the unit cell, which is in good agreement with the observed value of $4.56 \text{ g}\cdot\text{cm}^{-3}$ (Palache, Berman, and Frondel, 1955).

The integrated intensities were measured using the automatic diffractometer with Zr-filtered $\text{MoK}\alpha$ radiation (0.7107 Å). The intensities of 487 crystallographically independent reflections were measured within the range of $\sin \theta/\lambda < 0.5$ by the ω - 2θ scan technique. The specimen was so small that 75 reflections had the intensities equal to or less than the background values, and were regarded to be zero in intensity. Reflections with $\sin \theta/\lambda > 0.5$ were not measured. The intensity data were converted into observed structure factors by applying the standard Lorentz and polarization corrections. The absorption correction was not made, because the linear absorption coefficient was 125 cm^{-1} and the maximum length of the specimen was 0.003 cm.

STRUCTURE DETERMINATION AND REFINEMENT

Bertaut (1953) proposed a crystal structure for the $4C$ -type monoclinic pyrrhotite based on the space group $F2/d$ (Fig. 1), but he did not give explicitly any atomic coordinates of the structure. In order to describe the atomic coordinates, the space group $F2/d$ is maintained and expressed by the following coordinate system (Fig. 2) throughout in this investigation:

origin at $\bar{1}$ on a 'diamond' glide plane d with a translation of $(a + c)/4$;
unique axis b ;
coordinates of equivalent positions:

$$(0, 0, 0; \frac{1}{2}, \frac{1}{2}, 0; \frac{1}{2}, 0, \frac{1}{2}; 0, \frac{1}{2}, \frac{1}{2}) + \\ x, y, z; \frac{1}{4} - x, y, \frac{1}{4} - z; \bar{x}, \bar{y}, \bar{z}; \frac{1}{4} + x, \bar{y}, \frac{1}{4} + z.$$

The geometrical structure factors for this system are as follows:

$$\begin{cases} h + l = 4n \\ h + k = 2n \end{cases} \quad A = 16 \cos 2\pi(hx + lz) \cos 2\pi ky, B = 0; \\ \begin{cases} h + l = 4n + 2 \\ h + k = 2n \end{cases} \quad A = -16 \sin 2\pi(hx + lz) \sin 2\pi ky, B = 0; \text{ and} \\ \begin{cases} h + l = 2n + 1 \\ \text{or} \\ h + k = 2n + 1 \end{cases} \quad A = B = 0$$

According to this system, the atomic coordinates of iron atoms determined by Bertaut are described as in Table 1 by fixing one of the vacant positions at $1/8, 1/8, 1/8$ (Fig. 1). The iron atoms in the filled layers are represented in this investigation by odd numbers [Fe(1) and Fe(3)] and those in the vacancy-containing layers are by even numbers [Fe(2) and Fe(4)]. For this arrangement of iron atoms, two alternative arrangements of sulfur atoms are possible, because there are two possible positions for sulfur layers in the closest packing relation with the iron layers. The atomic coordinates of sulfur atoms in one of the arrangements

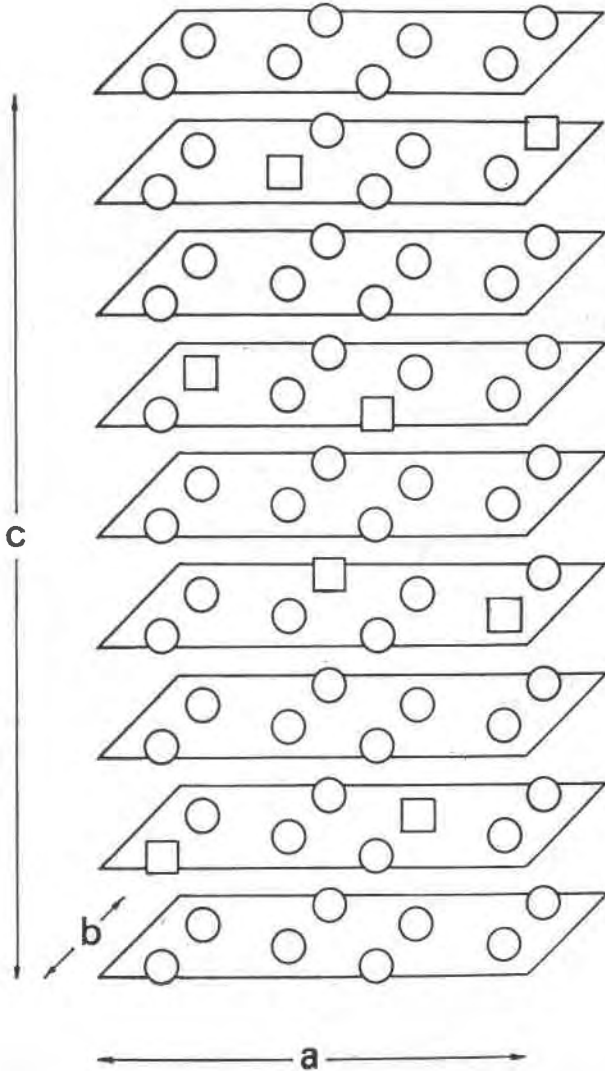
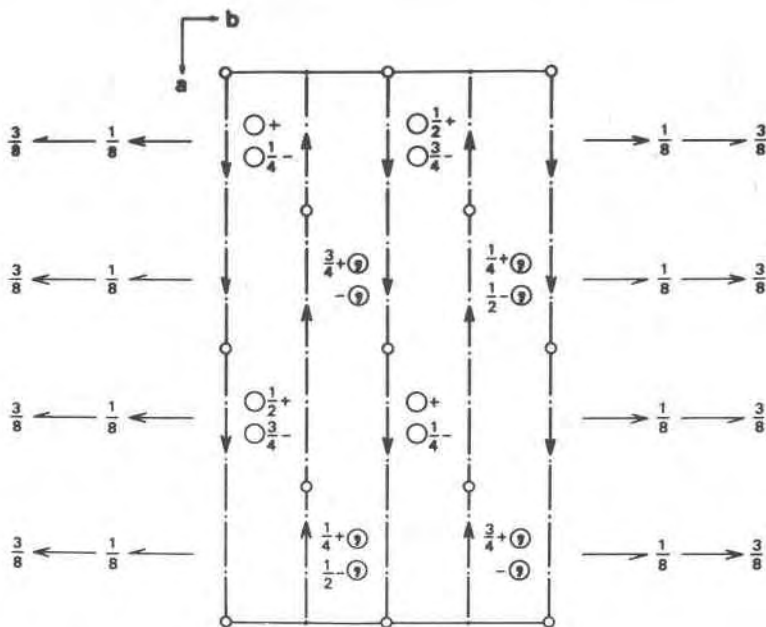


FIG. 1. The ideal structure of the 4C-type pyrrhotite proposed by Bertaut (1953) based on space group $F2/d$. Only iron layers are indicated and sulfur layers are omitted for simplicity. Squares represent vacant sites.

FIG. 2. Space group symmetry and equivalent positions of $F2/d$.

are listed in Table 1, while those in the other can be obtained by replacing (x, y, z) for sulfur atoms by $(1/4 - x, y, z)$ in Table 1. The choice between these two arrangements was carried out by comparison of F_o and F_c for hkl with $h = \pm 2 \pmod{6}$ and $l = \pm 4 \pmod{16}$, because the contributions of sulfur atoms to F_o of these reflections are same in absolute value but opposite in sign for these two alternatives. Because the atomic coordinates of sulfur atoms listed in Table 1 gave better agreement between F_o and F_c for the reflections mentioned above, they were determined to be correct ones for this structure.

Full matrix least-squares refinements of the structure were carried out on the FACOM 230-60 of Kyoto University with the use of RSFSL-4 of the UNICS system (Universal Crystallographic Computation System, Crystallographic Society of Japan, 1967) modified by Sakurai from ORFLS written by Busing, Martin, and

Table 1. Atomic coordinates of the $4C_2$ -type pyrrhotite (Fe_7S_8) based on the ideal structure proposed by Bertaut (1953).

	Number of equivalent points	Site symmetry	coordinate		
			x	y	z
Fe1	16	1	3/8	3/8	0
Fe2	16	1	3/8	3/8	1/8
Fe3	16	1	3/8	3/8	2/8
Fe4	8	2	3/8	3/8	3/8
S1	16	1	5/24	3/8	-1/16
S2	16	1	13/24	3/8	1/16
S3	16	1	5/24	3/8	3/16
S4	16	1	13/24	3/8	5/16

Levy (1962). The function minimized is $1/(\sigma)^2||F_o| - |F_c||^2$, where σ represents the estimated standard deviation computed from counting statistics. The estimated standard deviations of the weakest non-zero reflections were used for the reflections which were regarded as zero intensity. Scattering factors were taken from MacGillavry and Rieck (1962), assuming that sulfur atoms are doubly ionized and iron atoms are the mixture of 5/7 Fe^{2+} and 2/7 Fe^{3+} . Isotropic temperature factors were assumed as 1.0 for all atoms. Refinement was initiated using the atomic coordinates of the ideal structure (Table 1), with the arrangement of sulfur atoms described above, which gave $R = 0.395$.

The full matrix least-squares failed by divergence of the y coordinates when the x , y , and z coordinates were allowed to vary together. The first two cycles were, therefore, carried out with the fixed y coordinates varying only the x and z coordinates. In the next two cycles, all the x , y , z coordinates were allowed to vary. The final four cycles were carried out varying the atomic coordinates and isotropic temperature factors. The final R factors for all reflections and for reflections excluding zero intensity are 0.134 and 0.093, respectively. The final weighted R factor was 0.045. At this stage, the order of differences between F_o and F_c have become almost equal to the order of σF_o resulting in 1.69 for the quantity of error of fit, $[\sum_{N_o} \{(F_o - F_c)/\sigma F_o\}^2 / (N_o - N_p)]^{1/2}$, where N_o is the number of observed reflections and N_p the number of adjustable parameters. Any further refinement with increased number of parameters is, therefore, likely to result in no significant improvement. In fact, attempts to determine the ordering of ferric and ferrous ions in the structure or the anisotropic temperature factors for the atoms in the structure were not successful.

The final atomic coordinates and the individual isotropic temperature factors with the estimated standard deviations are given with the amount of displacements of atoms from the ideal structure (Table 2). F_o and F_c values are on deposit.¹

DESCRIPTION OF THE STRUCTURE

The interatomic distances and the bond angles (Table 3 and 4) were computed with the program RSDA-4 of the UNICS system (1967) based on the final atomic coordinates (Table 2). The estimated standard deviations of the atomic coordinates were used to compute the standard deviations in the interatomic distances and the bond angles.

Deviation from the ideal structure

The result of the refinement confirms the ideal structure proposed by Bertaut (1953). Sulfur atoms approximately occupy the nodes of the hexagonal closest packing and iron atoms are regularly arranged

¹To obtain a copy of this material, order NAPS Document Number 01805. The present address is National Auxiliary Publications Service of the A.S.I.S., c/o CCM Information Corporation, 866 Third Avenue, New York, New York 10022; and the price is \$2.00 for microfiche or \$5.00 for photocopies, payable in advance to CCMIC-NAPS. Check a recent issue of the journal for current address and price.

Table 2. Final atomic coordinates and isotropic temperature factors for atoms in pyrrhotite (Fe_7S_8) obtained in this study. Estimated standard deviations are in parentheses. The columns of $a \times |\Delta x|$, $b \times |\Delta y|$, and $c \times |\Delta z|$ indicate the amounts of displacement in Angstrom from the ideal structure proposed by Bertaut (1953).

	x	$a \times \Delta x $ (Å)	y	$b \times \Delta y $ (Å)	z	$c \times \Delta z $ (Å)	B
Fe1	0.3809(3)	0.070	0.3500 (9)	0.171	-0.0063(2)	0.144	0.94(10)
Fe2	0.3816(4)	0.079	0.3660(11)	0.062	0.1234(2)	0.036	0.89 (8)
Fe3	0.3587(3)	0.194	0.3975 (9)	0.154	0.2501(2)	0.002	0.75(10)
Fe4	0.3750		0.3528(12)	0.152	0.3750		1.41(13)
S1	0.2061(5)	0.026	0.3660(16)	0.062	-0.0618(3)	0.016	0.78(15)
S2	0.5418(6)	0.001	0.3833(15)	0.057	0.0598(3)	0.062	0.61(14)
S3	0.2096(5)	0.015	0.3858(15)	0.074	0.1805(3)	0.160	0.50(14)
S4	0.5428(5)	0.013	0.3645(15)	0.072	0.3087(3)	0.087	0.65(15)

in the octahedral interstices of the sulfur atoms. The vacancies among the iron sites are in ordered arrangement and confined to alternate layers of iron atoms and normal to the c axis (Fig. 1). These vacancies result in slight displacements of iron and sulfur atoms from the positions in the ideal structure proposed by Bertaut (Table 1). The amounts of displacement of atoms in the final structure are given in Angström along the a , b , and c axes (Table 2).

Coordinations of iron and sulfur atoms

Because of the ordering of vacant sites for iron atoms and the displacements of iron and sulfur atoms from the ideal structure, coordinations of iron and sulfur atoms indicate some characteristics in the structure under discussion in comparison with the structures of troilite (Evans, 1970) and of the 3C-type pyrrhotite (Fleet, 1971).

All the iron atoms lie between six sulfur atoms with octahedral arrangements and also between other iron atoms, which are so close that the iron atoms are coordinated both by sulfur atoms and by iron atoms as described later in detail.

The bond lengths and the bond angles around the iron atoms (Table 3) indicate that the octahedra of sulfur atoms are not much distorted in this structure. The mean distances of Fe—S are 2.446, 2.449, 2.456, and 2.444 Å for the octahedra of Fe(1), Fe(2), Fe(3), and Fe(4), respectively. These values are compared with the corresponding ones of 2.491 Å in troilite (Evans, 1970) and 2.448 Å in the 3C-type pyrrhotite (Fleet, 1971).

All the Fe—Fe distances are more than 3.1 Å in the basal iron layers except the Fe(3)—Fe(3) distance with 2.944 Å in the filled layer (Table 4). This makes a clear contrast with the structure of troilite, where the formation of triangular groups is characteristic in every basal iron layer with the Fe—Fe distance of 2.919 Å (Evans, 1970). However, the Fe—Fe distances between the neighboring iron layers are rather short along the c axis in the 4C-type structure, ranging from 2.868 to 2.956 Å (Table 3). They show systematic change along the c

Table 3. Interatomic distances (Å) and bond angles (°) in the 4C-type pyrrhotite (Fe₇S₈). Estimated standard deviations are in parentheses. The atomic coordinates of the iron atoms are given in Table 2. The sulfur atoms are distinguished by their z-coordinates as follows: \bar{A} , $\bar{z}_A=1/16$; \bar{B} , $\bar{z}_B=3/16$; \bar{C} , $\bar{z}_C=5/16$; \bar{D} , $\bar{z}_D=7/16$.

1) Fe1 polyhedron		2) Fe2 polyhedron		3) Fe3 polyhedron		4) Fe4 polyhedron	
Interatomic distances		Interatomic distances		Interatomic distances		Interatomic distances	
Fe1 - S1a	2.427(8)	Fe2 - S1C	2.449(10)	Fe3 - S1C	2.449(11)	Fe4 - S2d	2.404(10)
Fe1 - S4a	2.386(10)	Fe2 - S3C	2.369(10)	Fe3 - S3C	2.369(08)	Fe4 - S3d	2.410(10)
Fe1 - S3a	2.363(10)	Fe2 - S4C	2.535(10)	Fe3 - S4C	2.535(10)	Fe4 - S4d	2.517(07)
Fe1 - S1b	2.386(10)	Fe2 - S2C	2.493(10)	Fe3 - S3a	2.322(09)	Fe4 - Fe3	2.868(4)
Fe1 - S2b	2.438(8)	Fe2 - S3a	2.322(09)	Fe3 - S4a	2.565(08)		
Fe1 - S4b	2.674(10)	Fe2 - S4a	2.565(08)	Fe3 - S2d	2.493(10)		
Fe1 - Fe2	2.956(6)	Fe2 - Fe3	2.911(6)	Fe3 - Fe2	2.911(6)		
		Fe2 - Fe1	2.956(6)	Fe3 - Fe3*	2.944(6)		
				Fe3 - Fe4	2.868(4)		
bond angles of Fe1 octahedron		bond angles of Fe2 octahedron		bond angles of Fe3 octahedron		bond angles of Fe3 octahedron	
S1a-Fe1-S2a	91.8(3)	S1b-Fe2-S3C	89.2(3)	S1C-Fe3-S3C	89.6(3)	S2d-Fe4-S2d	95.2(4)
S1a-Fe1-S3a	93.2(3)	S1b-Fe2-S4C	95.8(4)	S1C-Fe3-S4d	86.6(3)	S2d-Fe4-S3d	90.5(4)
S1a-Fe1-S1b	89.6(3)	S2b-Fe2-S1ba	91.4(3)	S1C-Fe3-S3d	98.0(4)	S2d-Fe4-S4d	88.6(3)
S1a-Fe1-S4b	85.2(3)	S2b-Fe2-S1C	92.3(3)	S1C-Fe3-S4d	87.2(3)	S3d-Fe4-S4d	89.5(3)
S2a-Fe1-S3a	93.2(3)	S2b-Fe2-S4C	97.3(3)	S3C-Fe3-S4C	88.3(3)	S3d-Fe4-S3d	83.8(4)
S2a-Fe1-S2b	85.5(3)	S4b-Fe2-S2b	86.8(3)	S3C-Fe3-S3d	102.3(3)	S3d-Fe4-S3e	87.8(3)
S2a-Fe1-S1b	82.9(3)	S4b-Fe2-S1b	88.1(3)	S3C-Fe3-S2d	95.6(3)	S3d-Fe4-S2e	93.9(3)
S2a-Fe1-S4b	98.5(4)	S4b-Fe2-S1C	87.3(3)	S4C-Fe3-S2d	83.8(3)		
S3a-Fe1-S2b	97.3(3)	S4b-Fe2-S3C	85.7(3)	S4C-Fe3-S4d	79.3(3)		
S1b-Fe1-S2b	90.0(3)	S1C-Fe2-S3C	86.5(3)	S2d-Fe3-S3d	90.4(3)		
S1b-Fe1-S4b	85.4(3)	S3C-Fe2-S4C	90.2(3)	S2d-Fe3-S4d	85.6(3)		
S2b-Fe1-S4b	84.2(3)						
S1a-Fe1-S2b	169.4(4)	S1b-Fe2-S1C	173.9(4)	S1C-Fe3-S2d	169.0(3)	S3d-Fe4-S2e	173.3(4)
S2a-Fe1-S1b	168.1(4)	S2b-Fe2-S3C	172.4(4)	S3C-Fe3-S4d	167.4(3)	S4d-Fe4-S2e	176.3(5)
S3a-Fe1-S4b	175.7(3)	S4b-Fe2-S4C	174.3(4)	S4C-Fe3-S3d	168.4(3)		

* The coordinates of this Fe3 are (0.1413, 0.6025, 0.2499).

Table 4. Fe-Fe distances in the vacancy containing and filled iron layers. Estimated standard deviations are in parentheses. The iron atoms are located by the following letters: f, $x \approx 1/8$; g, $x \approx 3/8$; h, $x \approx 5/8$; i, $y \approx -1/8$; j, $y \approx 1/8$; k, $y \approx 5/8$; e, $y \approx 7/8$.

Vacancy-containing layer $z \approx 3/8$			Filled layer $z \approx 2/8$		
Fe4 -Fe2hj	3.263 (7)	Fe3-Felhk	3.678 (6)	Fe3 -Fe3hj	3.926 (6)
Fe4 -Fe2hk	3.613 (7)	Fe3-Felgk	3.109 (9)	Fe3 -Fe3fk	2.944 (6)
Fe2hj-Fe2hk	3.434 (11)	Fe3-Felfj	3.201 (6)	Felhk-Felgl	3.418 (6)
		Fe3-Felgi	3.760 (9)	Felfj-Felgi	3.514 (7)

axis: 2.868 Å for the central Fe(4)—Fe(3) distance increases to 2.956 Å for the Fe(2)—Fe(1) distance through 2.911 Å for the Fe(3)—Fe(2) distance (Fig. 3). The linear arrangement of iron atoms along the *c* axis in the ideal NiAs structure (Table 1) can be compared with the slightly bent arrangement in this structure where the angles Fe(1)—Fe(2)—Fe(3), Fe(2)—Fe(3)—Fe(4), and Fe(3)—Fe(4)—Fe(3) are 174.06°, 166.05°, and 167.71°, respectively.

Because a bonding interaction is expected between iron atoms with interatomic distances of about 3.0 Å or less (Goodenough, 1962), Fe(1) is coordinated by one iron atom [Fe(2)] Fe(2), and Fe(4) by two iron atoms [Fe(2) by Fe(3) and Fe(4), and Fe(4) by two Fe(3)], and Fe(3) by three iron atoms [Fe(2), Fe(3), and Fe(4)], besides by the six sulfur atoms with octahedral arrangement described above (Figs. 3 and 4). The Fe—Fe bonding in this structure will be discussed later in more detail.

The sulfur atoms are coordinated by five iron atoms which are on the corners of a trigonal prism because of a vacant site on one of the corners. Only S(4) is coordinated by six iron atoms as in troilite (Fig. 3).

The structure as a whole can be described to be built up of chain elements of seven octahedra of sulfur atoms around iron atoms, elongating along the *c* axis, in which the octahedra are united by sharing two opposite faces. The chain elements thus formed are connected sideways by sharing edges with the neighboring ones (Fig. 3).

Atomic arrangement around the vacant site

Vacant sites for iron atoms are orderly distributed in the vacancy-containing basal layers, and are surrounded by six sulfur atoms and two iron atoms. It is of interest to examine the arrangement of these neighboring atoms around the vacant sites. The amount of displacements of these neighbors from the positions in the ideal structure are

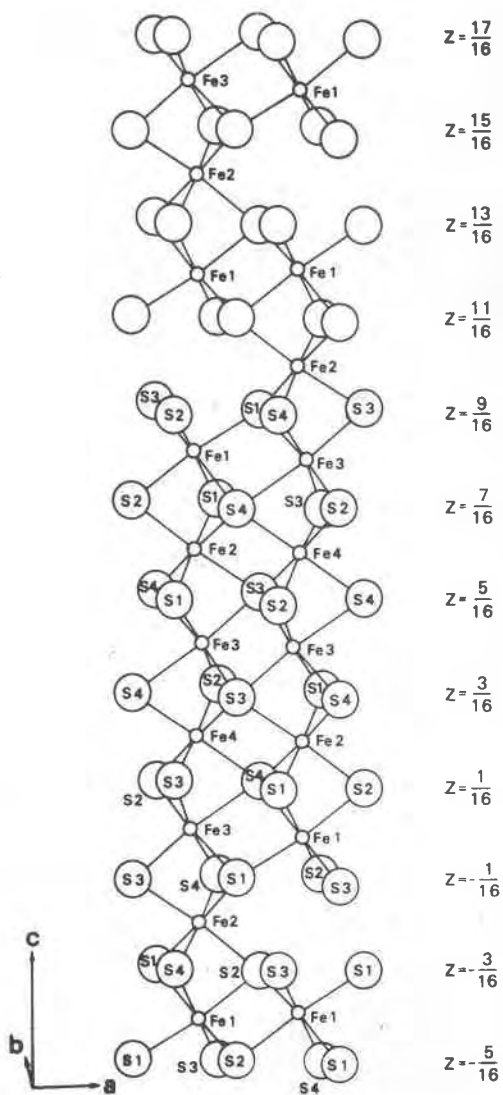


FIG. 3. Schematic drawing of the crystal structure of the 4C-type pyrrhotite. A group of seven octahedra of sulfur atoms around iron atoms builds a collective unit along the *c* axis, in which the octahedra are united by sharing two opposite faces.

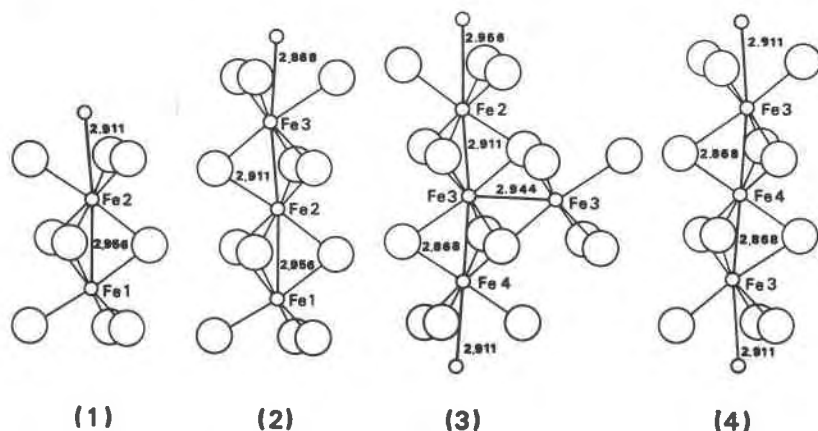


FIG. 4. The coordination schemes of iron atoms in the 4C-type pyrrhotite.

schematically shown in Figure 5, where the arrows represent the components of the displacements along the a , b , and c axes.

In order to compare the atomic arrangement around the vacant site with that around the iron atoms in the structure, a hypothetical site (X) was determined from the positions of octahedral sulfur atoms around the vacant site so that all the $X-S$ distances become approximately same. The coordinates of the X site were obtained to be (0.3750, 0.3668, -0.1250). The mean values for the $X-S$, $X-Fe$, and $S-S$ distances around the X site are compared with those for the $Fe-S$, $Fe-Fe$, and $S-S$ distances around the iron atoms (Table 5). The result seems to indicate that the octahedra of sulfur atoms around the vacant sites are only slightly smaller in comparison with those around the iron atoms. The $X-Fe$ distance is, however, significantly smaller than the $Fe-Fe$ distances.

DISCUSSION

Because the vacant sites are distributed in the structure as far as possible from each other and the atoms around the vacant sites are likely to move to reduce the vacant space, the structure of the 4C-type pyrrhotite seems to be essentially ionic.

In order to obtain a clue to the distribution of Fe^{2+} and Fe^{3+} , the stabilization energies have been calculated for different distributions of Fe^{3+} and Fe^{2+} on the basis of the refined structure. The distributions of Fe^{3+} were limited into the following four typical models after Bertaut (1953),

model 1 (distribution of $\text{Fe}^{2.29+}$ at all the iron sites),
 model 2 (distribution of Fe^{3+} at the Fe(2) sites),
 model 3 (distribution of Fe^{3+} at the Fe(1) sites) and
 model 4 (distribution of Fe^{3+} at the Fe(4) sites and a part
 of the Fe(1) sites).

The calculations were carried out by using a Madelung constant program (Unpublished report by Quintin Johnson of the Lawrence Radiation Laboratory, 1965) adapted to FACOM 230-60 computer at Kyoto University. The stabilization energies are as follows:

model 1	-276.3 kcal/mol,
model 2	-395.6 kcal/mol,
model 3	-409.9 kcal/mol and
model 4	-408.5 kcal/mol.

The conclusion that the model 3 is most stable among the four models is different from that obtained by Bertaut (1953) based on his ideal structure, which gave the stabilization energies of -495 kcal/mol for his model 4 and of -472 kcal/mol for his model 3. Our result seems reasonable because the electric unbalance caused by the vacancies of iron atoms can be compensated by the additional charge of Fe(1) atoms which are the nearest cations of the vacant sites.

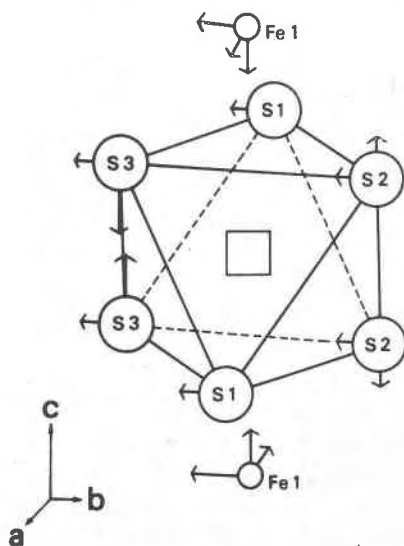


FIG. 5. Displacements of atoms around the vacant site from the positions in the ideal structure proposed by Bertaut (1953). The arrows represent the components of displacements along the a , b , and c axes.

Table 5. The mean distances (Å) for X-S, X-Fe and S-S around the vacant site (X) and those for Fe-S, Fe-Fe and S-S around iron atoms. Number in parentheses are those of bonds considered.

around X		around Fe1		around Fe2		around Fe3		around Fe4	
X-S(6)	2.439	Fe1-S(6)	2.446	Fe2-S(6)	2.449	Fe3-S(6)	2.456	Fe3-S(6)	2.444
S-S(12)	2.450	S-S(12)	3.450	S-S(12)	3.458	S-S(12)	3.457	S-S(12)	3.454
S-S(3)	4.876	S-S(3)	4.876	S-S(3)	4.889	S-S(3)	4.885	S-S(3)	4.881
X-Fe(2)	2.708	Fe1-Fe(1)	2.956	Fe2-Fe(2)	2.934	Fe3-Fe(3)	2.908	Fe4-Fe(2)	2.868

However, the Mössbauer spectra of the 4C-type pyrrhotite show no sign of Fe^{3+} even at 4.2°K (Hafner and Kalvius, 1966; Levinson and Treves, 1968). This means that even at this low temperature the Fe^{2+} and Fe^{3+} ions do not have separate existence for a time longer than that occupied by the Mössbauer transition (10^{-7} – 10^{-8} sec.). These results seem to reveal that the stability of pyrrhotite should be treated on the basis of an ionic model not of $\text{Fe}_5^{2+}\text{Fe}_2^{3+}\text{S}_8^{2-}$, but of $\text{Fe}_7^{2.29+}\text{S}_8^{2-}$ (model 1), although its calculated stabilization energy is not favorable.

Furthermore the observation of the Mössbauer spectra of the 4C-type pyrrhotite (Hafner and Kalvius, 1966; Levinson and Treves, 1968) provides three different magnetic fields at the sites of the iron atoms which are caused by the magnetic interactions between the iron neighbors in the structure. The application of an external magnetic field and the intensity ratio for the various subspectra indicate that the three different magnetic fields correspond to the Fe(2) and Fe(4), Fe(1) and Fe(3) (Levinson and Treves, 1968). Because the iron neighbors are different for these three kinds of iron atoms as explained above (Fig. 4), the structure obtained in this study explains well the results of the Mössbauer study.

According to Goodenough (1962), there are critical values of cation-cation separation below which the d -electron must be treated by means of collective system rather than localized one. In the Fe_{1-x}S system the critical separation is about 3.0 Å, (Goodenough, 1962). Accepting this critical value for the Fe-Fe separation, the group of seven iron atoms along the c axis can be considered as a collective unit in the 4C-type pyrrhotite (Fig. 3) like the triangular group in the troilite structure. Each iron group is connected with two others through the short Fe(3)-Fe(3) bonds in the filled iron layer, forming an endless chain elongated along [101] (Fig. 6). The formation of these iron clusters possibly increases the stability of the apparent ionic model of $\text{Fe}_7^{2.29+}\text{S}_8^{2-}$.

The complicated structure of iron clustering found in the 4C-type pyrrhotite must be important for understanding of the long-range ordering of vacant sites in the superstructures of pyrrhotite at various

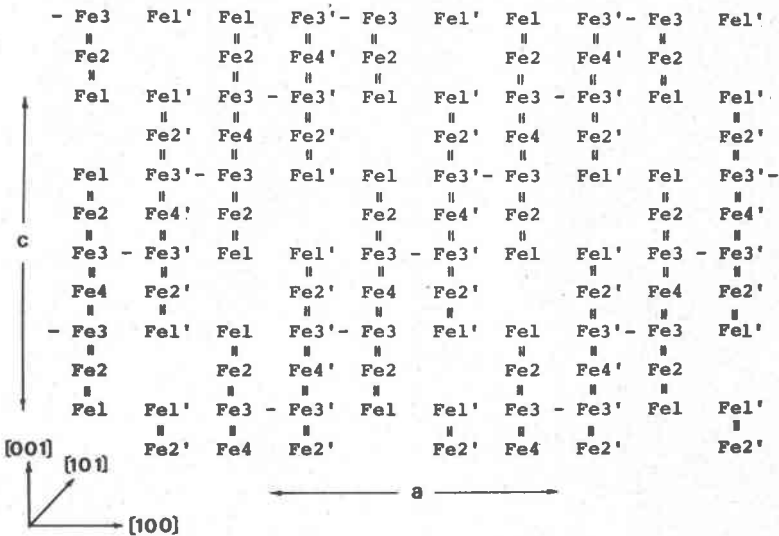


FIG. 6. Endless chains running parallel to [101] composed of chain elements of seven iron atoms elongated along the c axis.

temperatures and compositions (Morimoto, Nakazawa, Tokonami, and Nishiguchi, 1971; Nakazawa and Morimoto, 1971).

ACKNOWLEDGMENTS

We express our thanks to Dr. Mabel Corlett for providing us with the specimens from Kisbanya, Rumania, and to Dr. Quintin Johnson for providing us the Madelung Constant Program. Thanks are also due to Drs. H. Nakazawa and H. Horiuchi for illuminating discussions throughout this work, to Mr. A. Gyobu for drawing the figures, and to Miss M. Hirano for typing the manuscript.

REFERENCES

- BERTAUT, E. F. (1953) Contribution à l'étude des structures lacunaires. *Acta Crystallogr.* 6, 537-561.
- (1956) Structure de FeS stoechiométrique. *Bull. Soc. Franc. Mineral. Crystallogr.* 79, 276-292.
- BUSING, W. R., K. O. MARTIN, AND H. A. LEVY (1962) ORFLS, A Fortran Crystallographic Least-Squares Program. *U. S. Nat. Tech. Info. Serv. Rep. ORNL-TM-305*.
- CORLETT, MABEL (1968) Low-iron polymorphs in the pyrrhotite group. *Z. Kristallogr.* 126, 124-134.
- EVANS, H. T., JR. (1970) Lunar troilite: Crystallography. *Science*, 167, 621-623.
- FLEET, M. E. (1971) The crystal structure of a pyrrhotite (Fe_7S_8). *Acta Crystallogr.* B27, 1864-1867.
- GOODENOUGH, JOHN B. (1962) Cation-cation three-membered ring formation. *J. Appl. Phys.* 33, 1197-1199.

- HAFNER, STEFAN, AND MICHAEL KALVIUS (1966) The Mössbauer resonance of Fe^{57} in troilite (FeS) and pyrrhotite (Fe_{1-x}S). *Z. Kristallogr.* **123**, 443-458.
- MACGILLAVRY, C. H., AND G. D. RIECK (eds.) (1962) *International Tables for X-ray Crystallography, Vol. 3*, Kynoch Press, Birmingham.
- LEVINSON, LIONEL M., AND D. TREVES (1968) Mössbauer study of magnetic structure of Fe_7S_8 . *J. Phys. Chem. Solids*, **29**, 2227-2231.
- MORIMOTO, N., H. NAKAZAWA, K. NISHIGUCHI, AND M. TOKONAMI (1970) Pyrrhotites: Stoichiometric compounds with composition $\text{Fe}_{n-1}\text{S}_n$ ($n \geq 8$). *Science*, **168**, 964-966.
- , ———, M. TOKONAMI, AND K. NISHIGUCHI (1971) Pyrrhotites: Structure type and composition. *Soc. Mining Geol. Jap., Spec. Issue*, **2**, 15-21. [Proc. IMA-IAGOD Meeting '70. Joint-Symp. Vol.]
- NAKAZAWA, H., AND N. MORIMOTO (1971) Phase relations and superstructures of pyrrhotite, Fe_{1-x}S . *Mater. Res. Bull.* **6**, 345-358.
- PALACHE, C., H. BERMAN, AND C. FRONDEL (1955) *Dana's System of Mineralogy, Vol. 1*. John Wiley and Sons, New York, p. 233.
- WARD, J. C. (1970) The structure and properties of some iron sulfides. *Rev. Pure Appl. Chem.* **20**, 175-206.

Manuscript received, February 11, 1972; accepted for publication, February 25, 1972.